Final Report: Semi-Autonomous Control and Cyber-Pain for Artificial Muscles and Smart Structures (Award no.: FA2386-09-1-4087)

Date: 15 September 2010
From: Dr. Iain A. Anderson, Dr. Emilio Calius and Todd Gisby, Biomimetics Laboratory of the Auckland Bioengineering Institute, Level 6, 70 Symonds St., Auckland, New Zealand
Contact: i.anderson@auckland.ac.nz

Out of all the electro-active polymers, dielectric elastomer actuators (DEA) have characteristics that are the most similar to biological muscle, which is why they are also known as artificial muscles. The goal of this research was to establish the feasibility of using a cyber-pain signal to enable a DEA unit (comprising both an actuator and its local controller) to avoid some key failure modes. Our approach has built on our developments in dynamic self-sensing and realistic simulation of DEA electromechanics, including control circuits.

The achievements of this project can be summarized as

- design of a test DEA that encapsulated the critical failure modes;
- development of a novel monitoring circuit that incorporated our latest research into self-sensing algorithms;
- measurement of leakage currents and discharges across the dielectric, both of which are indicators of the state or condition of the dielectric elastomer devices; and
- correlation of DEA quality with the frequency of partial discharges.

In particular we have determined that the leakage current by itself is not a reliable predictor of impending failure, but the combination of partial discharge event frequency and leakage current noise is clearly correlated with damage processes in the artificial muscle. These indicators of damage were observed several seconds before full dielectric breakdown occurred, which indicates that it is possible to take corrective action by rebalancing loads and avoid failure.

This is an important step towards realizing the performance potential of dielectric elastomer devices. That is because the maximum electric field applied to a DEA is typically constrained by a large safety factor. For example, for DEA fabricated from VHB4905 a typical limiting value is 80MV/m. Based on our experiments, the worst performing DEA sustained an electric field 3 times higher before failing, which represents an active pressure 9 times greater than if a typical safety factor had been used. Clearly DEA performance could be increased by up to an order of magnitude if the applied field was controlled by a dynamic pain parameter instead of a static safety factor.

Several important avenues for future work arise from the results of our current experiments. The behaviour of the electrodes at very high strains suggests a means for measuring the equivalent series resistance of a DEA that will provide valuable feedback information. Resistance sensing will potentially enable the measurement of mechanical strain. It will also enable the voltage drop across the electrodes to be estimated, which we have to this point assumed to be negligible.

Project Milestones

The three project milestones are now complete, culminating in the production of a proof-of-concept pain-sensing DEA system. Each milestone is linked to an appended deliverable.

Milestone 1 – Comprehensive literature review (**Completed**)

Scientific significance: We have identified DEA failure mode data that exists and gaps in knowledge. This has helped us to produce a design for our test actuator and define the testing required.

Status: The competed report was sent to AOARD on 9 November 2009. The report is located in Appendix 1 on page 3.

Report Documentation Page

Form Approved
OMB No. 0704-0188

1. REPORT DATE	2. REPORT TYPE	3. DATES COVERED
23 SEP 2010	**Final**	**05-03-2009 to 17-09-2010**

4. TITLE AND SUBTITLE
Semi-Autonomous Control with Cyber-Pain for Artificial Muscles and Smart Structures

5a. CONTRACT NUMBER
FA23860914087

5b. GRANT NUMBER

5c. PROGRAM ELEMENT NUMBER

6. AUTHOR(S)
Iain Anderson

5d. PROJECT NUMBER

5e. TASK NUMBER

5f. WORK UNIT NUMBER

7. PERFORMING ORGANIZATION NAME(S) AND ADDRESS(ES)
Auckland Bioengineering Institute,Level 6, 70 Symonds St,Auckland 1142,New Zealand,NA,NA

8. PERFORMING ORGANIZATION REPORT NUMBER
N/A

9. SPONSORING/MONITORING AGENCY NAME(S) AND ADDRESS(ES)
AOARD, UNIT 45002, APO, AP, 96337-5002

10. SPONSOR/MONITOR'S ACRONYM(S)
AOARD-094087

11. SPONSOR/MONITOR'S REPORT NUMBER(S)

12. DISTRIBUTION/AVAILABILITY STATEMENT
Approved for public release; distribution unlimited

13. SUPPLEMENTARY NOTES

14. ABSTRACT

Dielectric elastomer actuators (DEA) have characteristics that are the most similar to biological muscle, which is why they are also known as artificial muscles. The goal of this research was to establish the feasibility of using a cyber-pain signal to enable a DEA unit (comprising both an actuator and its local controller) to avoid some key failure modes. Our approach has built on our developments in dynamic self-sensing and realistic simulation of DEA electro-mechanics, including control circuits. The achievements of this project can be summarized as ? design of a test DEA that encapsulated the critical failure modes ? development of a novel monitoring circuit that incorporated our latest research into self-sensing algorithms ? measurement of leakage currents and discharges across the dielectric, both of which are indicators of the state or condition of the dielectric elastomer devices; and ? correlation of DEA quality with the frequency of partial discharges.

15. SUBJECT TERMS

16. SECURITY CLASSIFICATION OF:			17. LIMITATION OF ABSTRACT	18. NUMBER OF PAGES	19a. NAME OF RESPONSIBLE PERSON
a. REPORT	b. ABSTRACT	c. THIS PAGE			
unclassified	**unclassified**	**unclassified**	**Same as Report (SAR)**	**28**	

Milestone 2 – Build actuators and obtain data to define pain parameters (**Completed**)

Scientific significance: We have determined the relevance of the three key variables: voltage, capacitance and leakage current in a pain parameter. Milestone steps have included:

- Designing an actuator for experiment
- Defining pain parameters
- Estimating required reaction time

Status: This work has been presented at conference and published in the following SPIE conference paper:

GISBY T.A., XIE S.Q., CALIUS E.P., and ANDERSON I.A., Leakage current as a predictor of failure in dielectric elastomer actuators, Electroactive Polymer Actuators and Devices (EAPAD), Yoseph Bar-Cohen(ed.), San Diego, Proc. SPIE, Vol 7642, Article number 7642-36, 2010.

This paper is located in Appendix 2, page 10.

Milestone 3- Build electronic hardware and define real-time pain-sensing algorithm. (**Completed**)

Scientific significance: We have demonstrated that the pain parameter can be detected in real time so that the actuation can be aborted before failure occurs. To achieve this we have:

- Designed and built electronic hardware
- Tested/demonstrated the hardware

Status: Our work that will soon be published is described in Appendix 3, page 19. This includes drawings of our pain-detection circuit. The publication is being prepared for presenting at the Electroactive Polymer Actuators and Devices (EAPAD), Conference, San Diego, March, 2011.

Appendix 1:
Literature review: Dielectric Elastomer Actuator Failure Modes

Introduction

The dielectric elastomer actuator (DEA) is a flexible capacitor consisting of an incompressible soft polymer membrane dielectric with compliant electrodes on both sides. Their muscle-like qualities include being capable of high energy densities and quiet operation whilst being flexible and having a low material density. When a voltage is applied the charge accumulating on the free faces gives rise to an electrostatic Maxwell pressure that results in out-of-plane compression and in-plane expansion. This is illustrated in Figure 1.

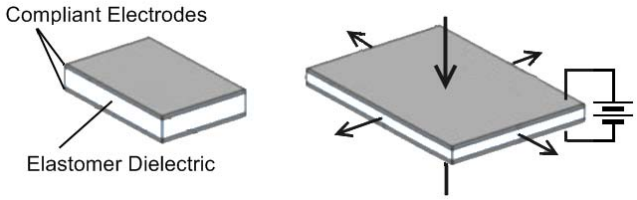

Figure 1: Basic planar DEA structure uncharged (left) and charged (right)

The Maxwell pressure is widely accepted to be defined by Equation 1 below [1]:

$$P = \varepsilon_r \varepsilon_0 E^2 \quad (1)$$

where P is the electrostatic Maxwell pressure, compressive in the thickness direction, ε_r is the relative permittivity of the dielectric material, ε_0 is the permittivity of free space (ε_0= 8.854 x 10^{-12} F/m) and E is the electric field strength with units of V/m. The thinner the membrane, the lower the voltage required to achieve a particular Maxwell pressure.

Thickness reduction can be achieved through pre-stretching the elastomer. For an incompressible material,

$$1 = \lambda_1 \lambda_2 \lambda_3 \quad (2)$$

where λ_i is the stretch ratio (final length/original length) in direction i. This can be rearranged to,

$$\lambda_1 = \frac{1}{\lambda_2 \lambda_3} \quad (3)$$

where the "1" direction is through the thickness. For example, when stretched by a factor of 3 in each planar direction (i.e. $\lambda_2 = \lambda_3 = 3$), the thickness of the dielectric membrane will be reduced by a factor of 9. Prestretching acrylic elastomers can also substantially boost the dielectric breakdown strength. This will be discussed in more detail below.

DEA actuators can be configured to work as membranes that expand in-plane (Figure 1) or contractile devices. The latter are typically stacked as a column (Figure 2).

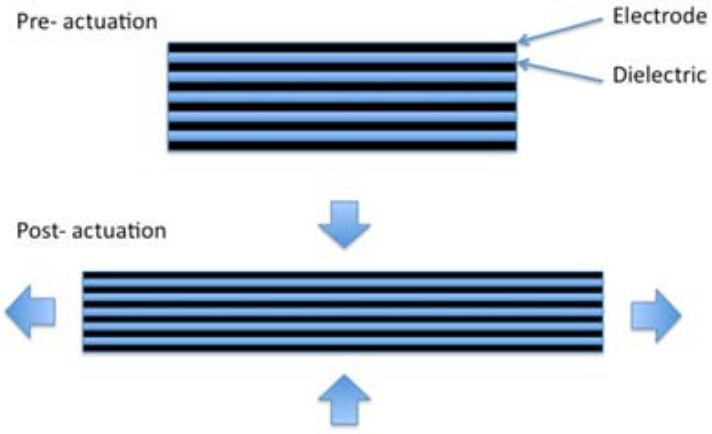

Figure 2: Basic contractile stacked actuator structure uncharged (top) and charged (bottom)

DEA Failure Modes

DEA have 4 primary modes of failure: tensile failure (Mode 1); dielectric breakdown (Mode 2); electromechanical instability (Mode 3); and buckling (Mode 4). These mechanisms can be interdependent. For instance, dielectric breakdown (Mode 3) may be initiated by the elastomer tearing (Mode 1), electromechanical instability (Mode 3), or buckling (Mode 4). An understanding of these modes of failure and how to avoid them is essential to the design of reliable actuator configurations and control protocols.

Mode 1: Tensile failure

DEA are constructed from soft, rubber-like materials that can undergo very large strains [4]. In its natural state long polymer backbones are entangled with intermittent cross-links tying neighbouring backbones together. The soft nature of these polymers comes from the relative ease that these chains can untangle and straighten out as the bulk material is stretched [5]. There is a limit to the amount of strain the material can sustain however, as at some threshold the chains will be fully straightened, and the presence of the cross links prevent chains from sliding past each other any further. At this point further strain will break the polymer backbone or cross-link, and if enough are broken the material will tear, i.e. tensile failure will occur.

Stress concentrations associated with the supporting framework of a DEA are a localised variation on tensile failure. In-plane configured DEA (see Figure 1) are typically supported in a frame that is much stiffer than the membrane itself. Careful consideration must be given to the interface between the membrane and the support. As the membrane deforms, the constraints imposed on the membrane by the frame can give rise to local stresses much higher than the nominal stress in the membrane. It is also important to ensure that the frame is free of sharp edges to prevent the membrane catching and tearing. If tensile failure occurs in one area of the membrane, the pre-strain will act to propagate the tear across the membrane.

Mode 2: Dielectric breakdown

The predominant failure mode of DEA is dielectric breakdown. Increased electrical conductivity as a result of dielectric breakdown leads to thermal runaway that permanently damages the DEA [6, 7]. Electrical conductivity through the thickness of the membrane increases with electric field, which generates heat within the membrane, causing the electrical conductivity to increase even further. Beyond some threshold heat will be generated in the core of the dielectric faster than it can be dissipated to the surrounding environment and a positive feedback loop will be formed. The resultant thermal runaway can damage the dielectric. Typically this will tend to occur at a weak point of the membrane e.g. around a defect such as a void or foreign particle trapped within the membrane.

Full dielectric breakdown results in catastrophic failure of the DEA, rendering it useless for future actuation, but it is possible for partial discharges to occur that do not cause catastrophic failure of the membrane. In a partial discharge, dielectric breakdown is initiated but a higher state of electrical conductivity is only maintained for a very short period of time. In the context of DEA there is evidence to suggest this results in dielectric ageing i.e. the membrane sustains damage but the actuator does not fail [8]. This effect can be harnessed to extend the operating life of the DEA. Yuang et. al. presented a fault tolerant DEA using carbon nanotube electrodes [8]. The electrodes locally degrade during dielectric breakdown, electrically isolating the faulty area. This action protects the DEA from catastrophic failure over multiple dielectric breakdowns.

The dielectric strength of membrane materials commonly used in DEA are given in Table 1 [9, 10].

Table 1: Dielectric strength of DEA dielectric materials.

Material	Dielectric Strength (MV/m)
VHB4910/4905	24.8
VHB4950/4930	18.1
Silicone Dow Corning Sylgard 186	17.7
Silicone Nusil CF19-2186	28.7
Air	3

It is well known that an increase in the dielectric strength of DEA can be achieved by prestretching them before actuation [11, 12]. For instance, the dielectric strength of VHB4910 was measured by Kofod at prestretches ranging from 0% to 500% equibiaxial stretch. When no prestretch was applied, the DEA broke down at an electric field of 17MV/m. At a prestretch of 500%, breakdown occurred under an electric field of 270MV/m [3]. Kornbluh et al have performed similar experiments and achieved a peak breakdown strength of 412MV/m for prestretched VHB 4910 and 350MV/m for prestrained Nusil CF19-2186 DEA [13].

Whilst no definitive conclusion has been reached in literature, it is widely suggested that enhancement of the breakdown strength by prestretch is related to the resultant changes in the macromolecular structure of the polymers [3, 14, 15]. Elastomers are an amorphous arrangement of polymer chains. When an elastomer is stretched, the chains align to the stress field. A schematic of this reorientation is given in Figure 3. In this case, the stress field is normal to the direction of the electric field. Free electrons move more readily along polymer chains than across them. Due to this alignment of the polymer chains, the free electrons are impeded from gaining enough energy to break other electrons free, increasing the field strength required to cause breakdown.

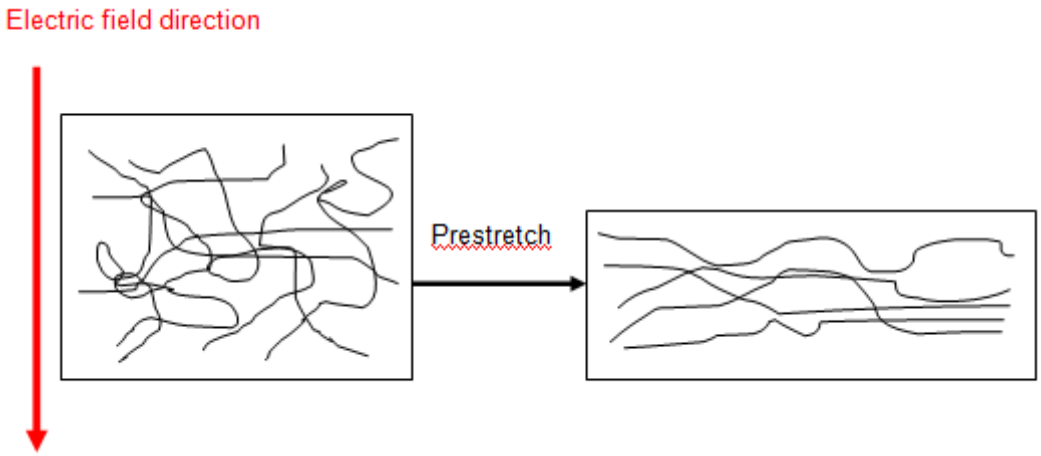

Figure 3: A cross section of an elastomer film before prestretching (left) and after prestretching (right).

Mode 3: Electromechanical instability

The deformation of a DEA finds an equilibrium point when the electric field generated stresses find a balance with the mechanical stresses in the membrane. The electrical and mechanical stresses however are interdependent; a change in the state of deformation of the DEA will affect the electric field and therefore electrostatic pressure acting on the DEA and vice versa.

Soft polymers are characterised by a hyperelastic stress-strain curve [5] as shown in Figure 4. The electric field generated pressure increases proportionately to the square of the electric field. For example, if an activated DEA is disturbed from its equilibrium position by an external out-of-plane compressive load or in-plane tensile load the membrane thickness will decrease. If charge is not removed from the DEA as it is deformed, the electric field and hence electrostatic pressure will increase (see Equation 1). With increasing electric field comes increasing electrostatic pressure, but, if this electrostatic pressure increases at a greater rate than the resisting stiffness of the

material, a positive feedback loop will be formed. The electrodes will attempt to clamp together. Failure occurs if in doing so the local stress exceeds the elongation at break of the material or if the electric field increases to the point of dielectric breakdown [16].

This can also be viewed in terms of energy i.e. the dielectric material is unable to develop enough strain energy to produce a state of equilibrium with the electrostatic energy. If the DEA is prestrained, then a greater amount of strain energy is developed for a given incremental increase in stretch. Reconsider the hyperelastic stress-strain curve in Figure 4. The area under the curve quantifies the strain energy of a deformation. The area shaded blue is the strain energy produced if an elastomer is deformed without prior prestretching. The area shaded red is the strain energy produced by straining the elastomer by the same amount after a prestrain of magnitude ε_{pre}. Thus pre-straining the dielectric will result in more elastic strain energy per unit deformation to resist the electrostatic strain energy.

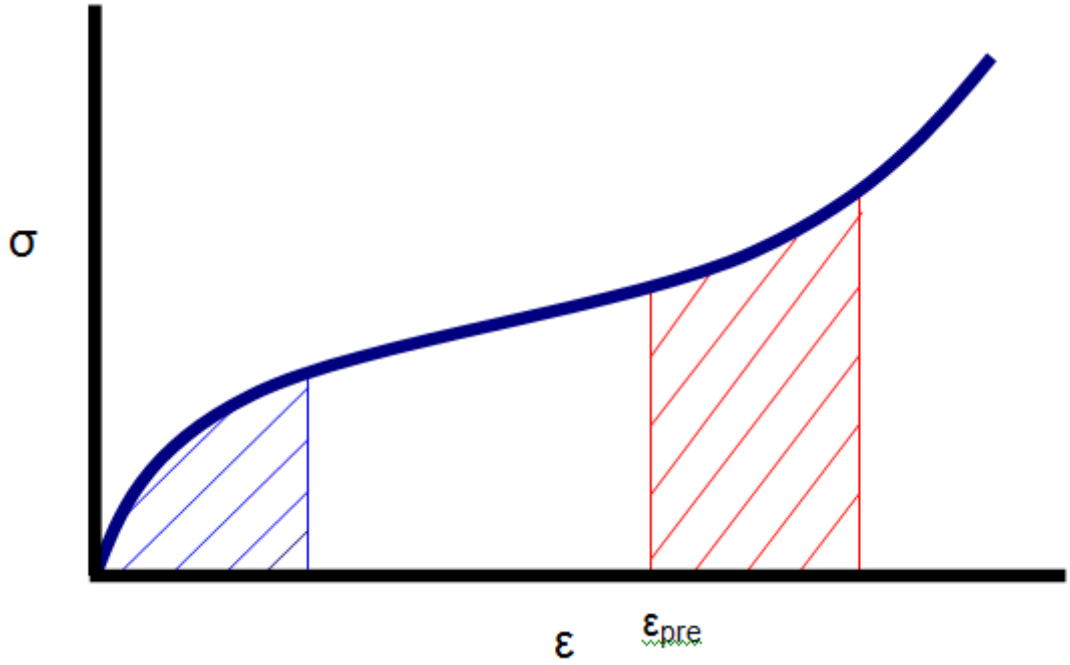

Figure 4: Hyperelastic stress (σ) vs strain (ε) curve illustrating the influence of prestraining on strain energy.

Mode 4: Buckling Mode Failure

Buckling mode failure occurs when the combined effect of the electrostatic and mechanical pressure act to generate compressive stresses in the plane of the membrane [17]. The membrane cannot sustain this compression and will subsequently collapse into a complex buckled state. Unlike the first three failure modes this does not necessarily result in catastrophic failure of the DEA, rather the loss in tension of the membrane will impair the DEA's ability to transmit force to a load. This can be a stable state for the DEA, however it is possible that the transition to the buckled state could satisfy the conditions required for one of the other failure modes to occur.

Mitigation of Failure Modes

The impressive performance of DEA is counterbalanced by their increased propensity for failure as they are driven close to their electromechanical limits. Without a means of actively avoiding these failures, there is a large gulf between the maximum level of actuation for reliable operation and the peak performance of a DEA. The approach that we are developing involves integrating sensing functionality into the DEA system. By monitoring the electrical characteristics of the DEA while it is being actuated, valuable information relating to not only the state of deformation of the DEA but also, we hope, to the health of the DEA can be extracted. A control system is being developed that will use this information to detect the onset of damage or degradation at the individual muscle level and respond appropriately. Much like the nervous system of an animal, this system is designed to fit into a distributed control structure where a centralized controller co-

ordinates the muscles towards an overall goal, while local controllers for individual muscle groups work to track the desired set-point whilst remaining within the capabilities of each muscle.

Perhaps the most obvious characteristic to monitor is DEA capacitance, which owing to the incompressible nature of the membrane can be used to infer the state of deformation of the DEA. We have experimentally validated simple capacitive sensing into an active DEA using a system based on Pulse Width Modulation (PWM) that exploits the difference between the electrical and mechanical time constants of a DEA [18]. By selecting a PWM frequency above the mechanical time constant of the DEA but below the electrical time constant, the mechanical system will see a relatively constant voltage (and hence electrostatic pressure) proportional to the duty cycle, while the amplitude of the high frequency signal on the electrical system can be used to infer the capacitance. At present this system relies on simplifying assumptions that ignore the effects of leakage current and a high rate of change of capacitance. An enhanced version that addresses these shortfalls has been developed and tested in simulation but not yet experimentally, compensating for the rate of change of capacitance effects and, even more importantly, allowing leakage current to be measured in real-time [19].

Capacitance is useful for combating tensile stress failures, buckling and electromechanical instability. The control system can use it to identify when the strain within the DEA is approaching the limits of the membrane material. It is also useful for identifying buckling, as in the event of a non-destructive collapse into the complex buckling structure the capacitance of the DEA will increase sharply. Accurate and timely feedback regarding the capacitance of the DEA is also essential if an electrical charge-based control system is to be used. This is especially important because if the amount of charge can be controlled, electromechanical instability can be prevented. If a constant charge is maintained, and the DEA is disturbed such that the membrane thickness is reduced, the incompressibility of the membrane means the electric field will actually decrease thereby reducing the electrostatic pressure and preventing the development of instability.

Careful design of the DEA will also serve to improve its reliability. Finite element analysis (FEA) modelling of the DEA and its support frame can identify high stress regions in both the active and passive regions of the membrane [20]. The degree of pre-stretch locked into the membrane will also affect reliability. As well as improving dielectric breakdown strength, it has been shown using an Ogden strain energy function model [21] that increasing pre-strain means the thickness can contract further before reaching a critical stability point, beyond which the electrodes will want to clamp together (i.e. electromechanical instability) [11].

The fabrication process used to produce DEA is also very important with regard to reliability. In DEA, dielectric breakdown often occurs at material defects. Micro-voids, foreign particles, and localised variations in the membrane thickness act as weak points in the dielectric. In this case, the onset of dielectric breakdown can be delayed by producing multilayer dielectrics, as placing two defects on top of each other is unlikely, thus the conduction path at the defect is blocked by the second dielectric layer [3].

At this stage of the project we are focussing on discovering the relationship between leakage current and dielectric breakdown. A method has been tested in simulation that allows leakage current to be separated in real-time from currents induced due to charging/discharging of the DEA and redistribution of charge due to a non-zero rate of change of capacitance. In combination with other measureable electrical characteristics of the DEA (e.g. capacitance, voltage) we are investigating the development of a parameter analogous to pain (i.e. a mechanism to predict impending failure) such that it can be used to prevent the DEA from being overexerted to the point of failing.

References

1. Pelrine, R.E., R.D. Kornbluh, and J.P. Joseph, *Electrostriction of polymer dielectrics with compliant electrodes as a means of actuation.* Sensors and Actuators, A: Physical, 1998. **64**(1): p. 77-85.
2. Plante, J.S., *Dielectric Elastomer Actuators for Binary Robotics and Mechatronics*, in *Department of Mechanical Engineering*. 2006, Massachusetts Institute of Technology: Boston.
3. Kofod, G., *Dielectric elastomer actuators*, in *The Department of Chemistry*. 2001, Technical University of Denmark.
4. Pelrine, R., et al., *High-speed electrically actuated elastomers with strain greater than 100%*. Science, 2000. **287**(5454): p. 836-9.
5. Boyce, M.C. and E.M. Arruda, *Constitutive models of rubber elasticity: A review*. Rubber Chemistry and Technology, 2000. **73**(3): p. 504-523.
6. Qi, X., Z. Zheng, and S. Boggs. *Computation of electro-thermal breakdown of polymer films*. in *2003 Annual Report Conference on Electrical Insulation and Dielectric Phenomena*. 2003: IEEE.
7. Dissado, L.A. and J.C. Fothergill, *Electrical degradation and breakdown in polymers.* Electrical Degradation and Breakdown in Polymers, 1992.
8. Yuan, W., et al. *Self-clearable carbon nanotube electrodes for improved performance of dielectric elastomer actuators*. in *Electroactive Polymer Actuators and Devices (EAPAD) 2008*. 2008. San Diego, California, USA: SPIE.
9. 3M, *VHB Tapes: Technical Data*. 2005, 3M Centre: St. Paul, MN.
10. Pelrine, R., et al., *High-field deformation of elastomeric dielectrics for actuators.* Materials Science and Engineering: C, 2000. **11**(2): p. 89-100.
11. Bauer, S. and M. Paajanen. *Electromechanical characterization and measurement protocol for dielectric elastomer actuators*. in *Smart Structures and Materials 2006: Electroactive Polymer Actuators and Devices (EAPAD)*. 2006. San Diego, CA, USA: SPIE.
12. Madden, J.D., et al., *Artificial Muscle Technology: Physical Principles and Naval Prospects*. 2003, The University of British Columbia: Vancouver.
13. Kornbluh, R.D., et al. *Ultrahigh strain response of field-actuated elastomeric polymers*. in *Smart Structures and Materials 2000: Electroactive Polymer Actuators and Devices (EAPAD)*. 2000. Newport Beach, CA, USA: SPIE.
14. O'Halloran, A. and F. O'Malley, *Materials and Technologies for Artificial Muscle: A Review for the Mechatronic Muscle Project*, in *Topics in Bio-Mechanical Engineering*, P.J. Prendergast and P.E. McHugh, Editors. 2004, Trinity Centre for Bioengineering & National Centre for Biomedical Engineering Science.: Galway. p. 184-215.
15. Taylor, D.M., *ESD: The Problems it Causes in Electronics*, School of Electronic Engineering Science, University College of North Wales: Bangor. p. 5.
16. Plante, J.-S. and S. Dubowsky. *On the nature of Dielectric Elastomer actuators and its implications for their design*. 2006. San Diego, CA, United States: International Society for Optical Engineering, Bellingham WA, WA 98227-0010, United States.
17. Zhou, J., et al., *Propogation of Instability in Dielectric Elastomers.* International Journal of Solids and Structures, 2008.
18. Gisby, T.A., et al. *An adaptive control method for dielectric elastomer devices*. in *Electroactive Polymer Actuators and Devices (EAPAD) 2008*. 2008. San Diego, California, USA: SPIE.
19. Gisby, T.A., et al. *Integrated sensing and actuation of muscle-like actuators*. in *Electroactive Polymer Actuators and Devices (EAPAD) 2009*. 2009. San Diego, CA, USA: SPIE.
20. O'Brien, B., et al., *Finite element modelling of dielectric elastomer minimum energy structures.* Applied Physics A: Materials Science & Processing, 2008.

21. Ogden, R.W., *Large Deformation Isotropic Elasticity - On the Correlation of Theory and Experiment for Incompressible Rubberlike Solids.* Proceedings of the Royal Society of London. Series A, Mathematical and Physical Sciences, 1972. **326**(1567): p. 565-584.
22. Laurent, C. and G. Teyssedre, *Hot electron and partial-discharge induced ageing of polymers.* Nuclear Instruments and Methods in Physics Research, Section B: Beam Interactions with Materials and Atoms, 2003. **208**(1-4): p. 442-447.

Appendix 2:

Here we have appended our conference paper presented to Electroactive Polymer Actuators and Devices (EAPAD), Yoseph Bar-Cohen(ed.), San Diego, Proc. SPIE, Vol 7642, Article number 7642-36, 2010.

Leakage current as a predictor of failure in Dielectric Elastomer Actuators

T. A. Gisby[1a], S. Q. Xie[b], E. P. Calius[c], I. A. Anderson[a]
[a]Biomimetics Laboratory, Auckland Bioengineering Institute, University of Auckland, 70 Symonds Street, Auckland, NZ
[b]Department of Mechanical Engineering, School of Engineering, The University of Auckland, Private Bag 92019, Auckland Mail Centre, Auckland 1142, NZ
[c]Industrial Research Limited, Brooke House, 24 Balfour Road, PO Box 2225, Auckland 1140, NZ

ABSTRACT

Dielectric breakdown often leads to catastrophic failure in Dielectric Elastomer Actuator(s) (DEA). The resultant damage to the dielectric membrane renders the DEA useless for future actuation, and in extreme cases the sudden discharge of energy during breakdown can present a serious fire risk. The breakdown strength of DEA however is heavily dependent on the presence of microscopic defects in the membrane giving its overall breakdown strength inherent variability. The practical consequence is that DEA normally have to be operated far below their maximum performance in order to achieve consistent reliability.

Predicting when DEA are about to suffer breakdown based on feedback will enable significant increase in effective DEA performance without sacrificing reliability. It has been previously suggested that changes in the leakage current can be a harbinger of dielectric breakdown; leakage current exhibits a sharp increase during breakdown. In this paper the relationship between electric field and leakage current is investigated for simple VHB4905-based DEA. Particular emphasis is placed on the behaviour of leakage current leading up to and during breakdown conditions. For a sample size of nine expanding dot DEA, the DEA that failed at electric fields below the maximum tested exhibited noticeably higher nominal power dissipation and a higher frequency of partial discharge events than the DEA that did not breakdown during testing. This effect could easily be seen at electric fields well below that at which the worst performing DEA failed.

Keywords: Dielectric Elastomer Actuators, leakage current, failure, dielectric breakdown

INTRODUCTION

Dielectric Elastomer Actuators (DEA) are soft, lightweight actuators that have demonstrated remarkable performance characteristics in terms of active stress, strain, strain rate, energy density and electromechanical efficiency[1]. They show great promise as an engineering analogue to natural muscle. There is a large difference however between the peak performance that has been recorded in laboratory conditions and what is realistically achievable during reliable operation. Performance of a DEA is limited by the maximum electric field it can sustain without undergoing electrical breakdown, a characteristic that varies between DEA due to the microscopic variability in the chemical structure inherent to polymer materials. It is highly desirable therefore to find some way of detecting the precursors to dielectric breakdown in a timely manner such that it can be prevented. To the best of the authors' knowledge a real time system for predicting and preventing dielectric breakdown in DEA has not been published.

DEA consist of a highly compliant incompressible polymer membrane dielectric sandwiched between compliant electrodes (Figure 5). When a voltage is applied to a DEA, the electrical charge that accumulates generates a surface pressure that results in a through thickness compression and in-plane expansion of the membrane. If the planar dimensions of the DEA are much greater than its thickness, the magnitude of the pressure is defined by Equation 1. P is the pressure, ε_r is the relative permittivity of the dielectric material, ε_0 is the permittivity of free space (8.854×10^{-12}F/m), V is the voltage, and d is the dielectric membrane thickness in meters[2].

*Author to whom correspondence should be addressed: t.gisby@auckland.ac.nz

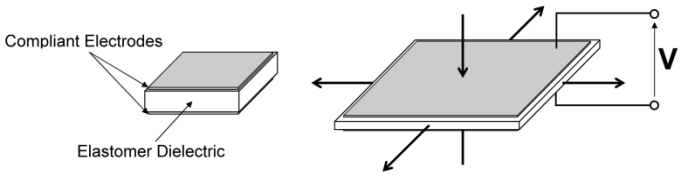

Figure 5: Actuation process of a basic DEA

$$P = \varepsilon_r \varepsilon_0 \left(\frac{V}{d}\right)^2 \quad (1)$$

The maximum pressure is governed by the maximum electric field the dielectric can sustain without undergoing breakdown. There are four mechanisms by which full dielectric breakdown is initiated[3]: electrical, the ideal breakdown strength of a material; electromechanical, where the mechanical stresses in the membrane are overpowered by the electrostatic pressure and the electrodes clamp together; thermal, where the leakage current generates enough heat to damage the dielectric; and partial discharge, where numerous partial discharges gradually weaken the dielectric to the point that full dielectric breakdown occurs. However, irrespective of the mechanism, the result of breakdown is thermal runaway[3]. At high electric fields leakage current through the dielectric causes its temperature to increase. As the temperature rises so too does the conductivity of the membrane, further increasing the leakage current. Beyond some threshold positive feedback occurs. For a DEA this is catastrophic; the heat generated by the runaway current melts/vaporizes the dielectric and creates a low-breakdown path between the electrodes. This subsequently prevents the electric field from reaching a level sufficient for significant actuation.

Pre-determining the breakdown strength of a DEA is a challenging task because of the inherent variability in the characteristics of the dielectric membrane. Membrane imperfections are unavoidable; for example micro-voids or impurities introduced during fabrication act as weak points in the dielectric. Similarly variations in the molecular structure and polymer chain density of the membrane result in spatial variations in the membrane's electronic properties. Dielectric breakdown therefore is typically a localized phenomenon, not unlike fatigue cracking in structural materials. Because of these imperfections it is unlikely a DEA will reach its ideal breakdown strength. The risk of electromechanical breakdown can be avoided if the DEA membrane is pre-stretched[4], or charge control is used[5]. For a DEA therefore it is most likely that full breakdown is primarily the result of thermal runaway or accumulated partial discharge damage.

Thermal breakdown occurs when the leakage current generates heat in the dielectric membrane faster than it can be dissipated to the surrounding environment. A positive feedback loop will be formed if an equilibrium cannot be found between the heat input and heat output, and this will ultimately melt/vaporize the dielectric and create a low breakdown path between the electrodes. Partial discharge events are the result of inhomogeneities within the dielectric membrane that either come about from the fabrication process or as a result of mechanical deformation. Within a void for example, the lower relative permittivity serves to enhance the local electric field. Local breakdown within the void create charge carriers that are then accelerated across the void by the electric field and, if they acquire enough energy, may subsequently damage the void wall and make it larger. This does not immediately result in failure of the dielectric, but repeated partial discharges can ultimately weaken the dielectric sufficiently that full breakdown occurs.

One approach to the issue of dielectric breakdown is to use self-clearing electrodes[6]. The DEA can be preconditioned by applying an electric field above its maximum operating field to burn out the defects and give some confidence as to the reliability of the DEA during operation. This effectively guarantees a minimum level of performance assuming the characteristics of the membrane do not change over time, but is there some way we could determine when a DEA was being actuated at its true limits in real time?

In this paper the relationship between electric field and leakage current and dielectric breakdown is investigated for a simple VHB4905-based DEA. Particular emphasis is placed on the behaviour of leakage current during breakdown conditions and its potential to be part of a "pain" parameter for predicting breakdown in a timely manner. This is motivated by the recent development of a self-sensing method for DEA that allows leakage current to be measured independently of charging/discharging currents[5].

Methods

Nine expanding dot DEA were fabricated from sheets of 3M VHB4905 tape that were stretched equibiaxially to 16 times their original area and bonded to a rigid circular support frame (Figure 6). The frame had an internal aperture with a diameter of 100mm. In the centre of the stretched membrane a circular electrode of diameter 24mm was applied to opposing sides of the membrane using Nyogel 756 electrically conductive carbon loaded grease. Nyogel 756 tracks approximately 6mm wide were also applied radially out from the electrode area to the points on the edge of the support frame that could be connected to external circuitry.

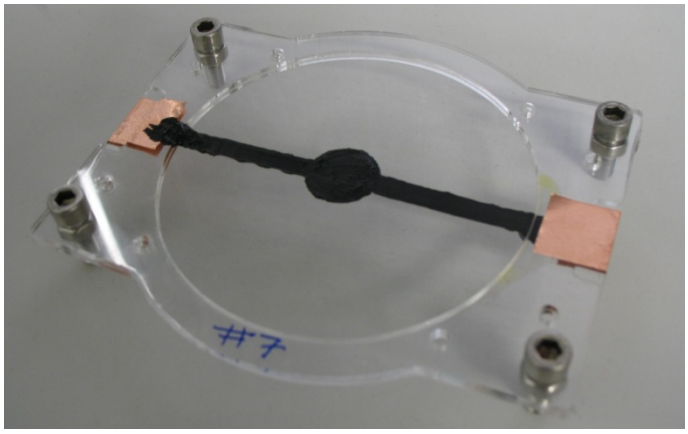

Figure 6: Simple expanding dot DEA and support frame

The relatively high resistance of the conductive tracks connecting the DEA to the edge of the support frame interfered with the ability of a commercially available RCL meter to accurately measure the rest capacitance and Equivalent Series Resistance (ESR) of the DEA. A custom Printed Circuit Board (PCB) amplifier was designed and fabricated in-house for calculating these rest values. A 10MΩ resistor was placed in series with the DEA between its negative electrode and ground to form a simple high-pass filter (Figure 7).

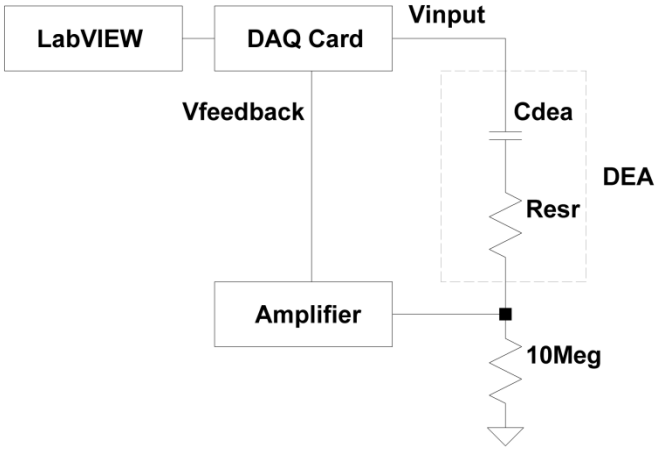

Figure 7: Schematic of system for measuring rest capacitance and rest equivalent series resistance of a DEA

A 2Hz, 20V peak-to-peak triangle wave voltage signal was applied to the positive electrode of the DEA and the current through the series resistor was measured using LabVIEW (8.6, National Instruments) via a PCIe-6259 DAQ card (National Instruments). Capacitance was calculated using the ratio of the instantaneous current to the rate of change of the voltage (Equation 2). To characterize the accuracy of this method three different fixed capacitors were tested with a Fluke RCL Meter (PM 6306A) and with the custom PCB and the results were compared. Each fixed capacitor was tested three times using the custom PCB to find an average value for capacitance. The error between this average value and the reading from the Fluke RCL Meter was calculated.

$$C = \frac{i}{\dot{V}} \tag{2}$$

Initially the ESR of the DEA was assumed to be zero and the cut-off frequency of the circuit formed by the capacitance of the DEA and the 10MΩ fixed resistor was estimated. The estimated cut-off frequency of each DEA fell within the range of 45-55Hz. A 6V peak-to-peak sine wave voltage signal with a frequency of 1kHz was then applied to the positive electrode of the DEA. The impedance of the capacitance at the applied frequency and the ratio of the amplitude of the input waveform to the amplitude of the feedback waveform were used to estimate the ESR of the DEA using Equation 3. X_{ESR} is the impedance of the electrodes, X_C is the impedance of the capacitor element, $X_{10M\Omega}$ is the impedance of the fixed resistor, A_{Vout} is the amplitude of the sinusoidal output waveform measured across the 10MΩ resistor, and A_{Vin} is the amplitude of the sinusoidal waveform applied to the positive terminal of the DEA.

$$X_{ESR} = \left(\sqrt{\frac{X_{10M\Omega}^{2}}{\left(\frac{A_{Vout}}{A_{Vin}}\right)^{2}} - X_C} \right) - X_{10M\Omega} \tag{3}$$

In order to examine the relationship between the leakage current and level of actuation during high voltage tests of each DEA a second PCB was designed and built to control the high voltages applied to the DEA. The same circuit from Figure 7 was used, with the addition of a 600:1 DC-DC converter that was used to amplify V_{input} before it was applied to the DEA. The buffered feedback signals were recorded using LabVIEW via the DAQ card.

The first step in each DEA test was to apply a voltage of 500V for 30 seconds. This voltage was chosen because of the minimum turn-on voltage of the DC-DC Converter (T-3005, AM Power Systems) used to generate the high voltages, and it was left for 30 seconds to ensure the DEA was at a stable equilibrium before the test began. At the end of this 30 second period the voltage was increased linearly at a rate of 5V/s to 3000V or until the DEA failed, whichever came first. This test procedure was initially performed without a DEA connected to the circuit in order to calibrate the voltage dependency of the feedback circuit. In post-processing of the acquired data this calibration curve was subtracted from the acquired data curve to get the true feedback measurements.

Each DEA was placed in a purpose built jig that allowed a video camera to look down on the circular electrode area whilst it was being actuated (Figure 8). Each experiment was recorded using the video camera, and the video was post-processed in order to measure the changes in the electrode area as the actuation level increased.

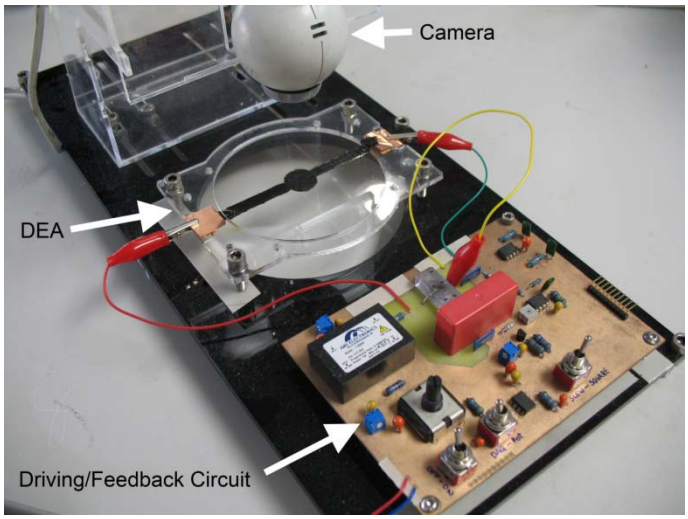

Figure 8: Experimental setup for leakage current testing

Post-processing of the data acquired from the experimental procedure was carried out using a purpose built DEA analysis script written in Matlab (R2008a, The MathWorks, Inc.). The video feedback was analysed on a frame-by-frame basis. The height of the camera and the resolution of each frame corresponded to a linear distance of approximately 200μm/pixel in both the height and width dimensions. A three stage process was applied to each frame: first, a threshold was applied to convert it to a binary image; second, the electrode tracks connecting the DEA to the edge of the support frame were measured and removed from the image; and third, the number of black pixels remaining (corresponding to the active area of the DEA) were counted and recorded against the time stamp of the frame (Figure 9). The relative size of the area of the DEA and the rest capacitance were used to calculate the instantaneous capacitance versus time, and this was differentiated to find the rate of change of capacitance versus time. This method precluded analysing the video feedback in real time due to the computational requirements.

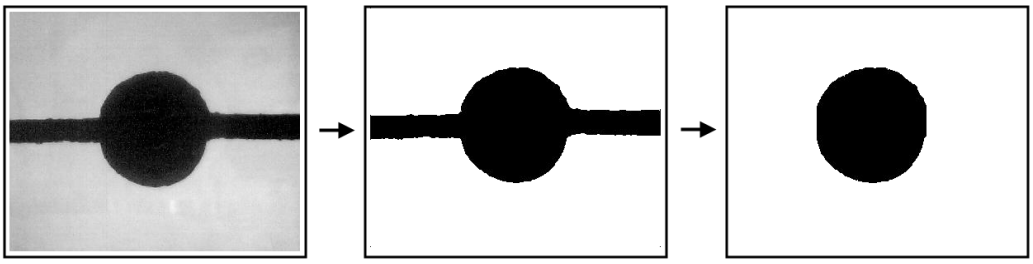

Figure 9: Frame-by-frame image processing sequence: raw image (left); thresholded binary image (center); and image containing only active region of the DEA (right)

The DEA analysis script also imported the voltage and series current feedback data and correlated it to the timescale of the video. Assuming the membrane to be incompressible, the change in the thickness of the membrane is inversely proportional to the stretch ratio of the electrode area. This instantaneous thickness estimate of the dielectric membrane was correlated with the recorded voltage data to calculate the instantaneous electric field.

The current measured through the series resistance is the sum of three constituent components: current due to the charging/discharging of the DEA's capacitance; current due to the redistribution of charge as the capacitance changes; and leakage current (Equation 4)[5].

$$i = C\dot{V} + \dot{C}V + i_{leakage} \tag{4}$$

The recorded series current was first corrected using the data obtained from the calibration run of the test setup. Capacitance and the rate of change of capacitance were extracted from the processed video feedback data. Voltage and the rate of change of voltage were extracted from the feedback data recorded using LabVIEW. These values were then used to calculate the true leakage current through the thickness of the membrane.

Once isolated, the characteristics of the leakage current were further analyzed using the DEA analysis script. A 4th order low pass Butterworth filter with a cut-off frequency of 10Hz was used to separate the nominal leakage current from the discharge events. This was then correlated with the electric field within the DEA and the area of the electrodes, and used to calculate the power per unit area that was being dissipated by the DEA (Equation 5). V_{DEA} is the voltage across the DEA, $i_{leakage}$ is the leakage current, r_0 is the initial radius of the DEA electrode area, and λ_{area} is the stretch ratio of the area (defined as the ratio of the instantaneous electrode area to the initial electrode area).

$$\frac{Power}{Area} = \frac{V_{DEA} i_{leakage}}{\pi r_0^2 \lambda_{area}} \tag{5}$$

A 4th order high pass filter with a cut-off frequency of 100Hz was then used on the leakage current data to remove the nominal leakage current and leave just the discharge events. A discharge event was deemed to have occurred if the high pass filtered current rose above 200nA. The magnitude and frequency of partial discharges was then correlated with the electric field.

RESULTS

The results of the calibration test for the capacitance meter are given in Table 1, and exhibit excellent agreement between the test instrumentation and the Fluke RCL meter. The rest capacitance and the rest ESR measurements for each of the nine DEA tested are shown in Table 2. In both tables the capacitance values have been rounded to the nearest picofarad.

Table 1: Calibration of DEA rest capacitance meter circuit

Capacitor	Fluke RCL Meter Reading	Custom PCB Capacitance Meter Readings				
		Reading 1	Reading 2	Reading 3	Average Reading	% Error
1	225pF	225pF	227pF	226pF	226pF	0.44
2	446pF	446pf	450pF	448pF	448pF	0.45
3	661pF	666pF	670pF	668pF	668pF	0.30

Table 2: Rest capacitance and rest equivalent series resistance of test DEA

DEA	Rest Capacitance				Rest Equivalent Series Resistance	
	Reading 1	Reading 2	Reading 3	Average Reading	V_{out}/V_{in}	R_{ESR}
A	301pF	303pF	301pF	302pF	0.93138	724kΩ
B	290pF	290pF	290pF	290pF	0.92517	795kΩ
C	290pF	288pF	289pF	289pF	0.93077	730kΩ
D	336pF	338pF	337pF	337pF	0.94578	563kΩ
E	287pF	288pF	287pF	287pF	0.93907	634kΩ
F	286pF	286pF	284pF	285pF	0.93898	635kΩ
G	302pF	303pF	302pF	302pF	0.94499	569kΩ
H	293pF	293pF	292pF	293pF	0.93050	733kΩ
I	288pF	286pF	284pF	286pF	0.92990	739kΩ

When subjected to the high voltage test, 6 of the 9 DEA failed during testing, and are denoted with solid lines in Figures 6, 7, 8, 10, and 11. The 3 DEA that did not fail are denoted with dashed lines in the same figures. Also note that data has been downsampled where appropriate to improve readability.

The instantaneous voltage across the DEA was correlated with its instantaneous thickness to calculate the electric field. Electric field versus the area stretch ratio is shown in Figure 10. Electric field versus the nominal leakage current is shown in Figure 11. Electric field versus the power dissipated per square meter is shown in Figure 12.

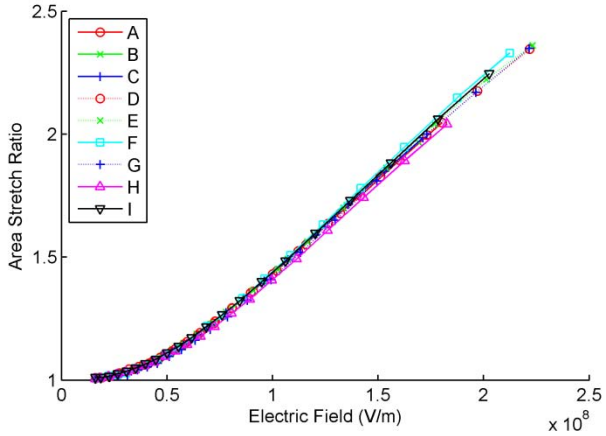

Figure 10: Area stretch ratio versus electric field for the 9 DEA tested

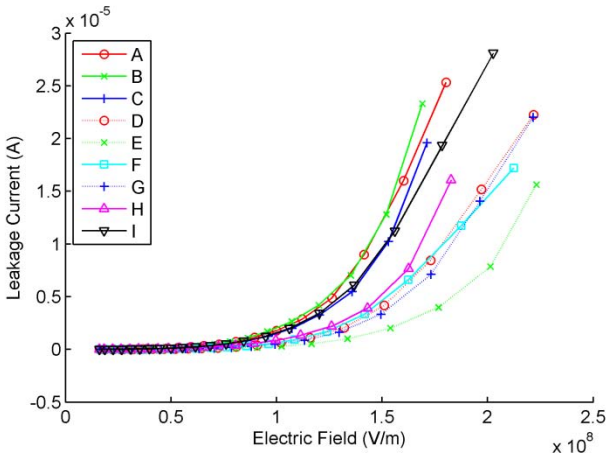

Figure 11: Nominal leakage current versus electric field for the 9 DEA tested

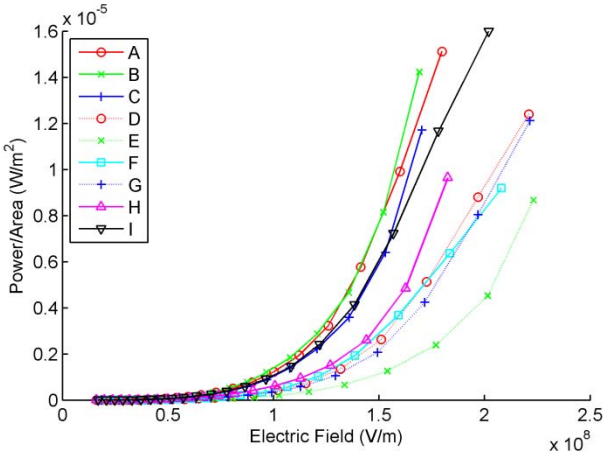

Figure 12: Power dissipated per square meter versus electric field for the 9 DEA tested

The leakage current data was also analyzed to identify the frequency of discharges due to partial breakdowns in relation to the electric field. A typical leakage current plot for a single test is shown in Figure 13. Note the clean shape of the underside of the characteristic leakage current curve that indicates that the spikes in the signal correspond to partial discharges and are not artifacts as a result of noise in the feedback circuit. The number of spikes in the leakage current data were counted for each second of the test and correlated with electric field and a third order polynomial was fit to the resultant data using Matlab's 'polyfit' function (Figure 14). The magnitude of the partial discharge was also measured. This was averaged on a second-by-second basis and correlated with the electric field. Two representative curves are shown in Figure 15: one from a DEA that did not break down during testing (Sample E); and one from a DEA that did break down (Sample I). Whilst some variability existed, the DEA that did not fail had similar characteristics to that of Sample E i.e. relatively large, but less frequent partial discharges. Similarly, Sample I was

representative of the general characteristics of the DEA that failed during testing i.e. much smaller but much more frequent partial discharges.

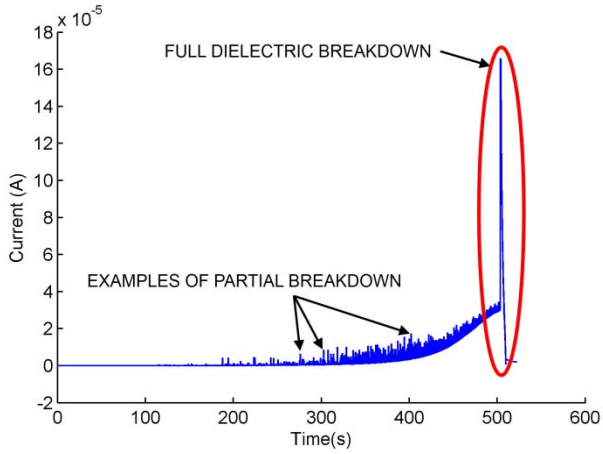

Figure 13: Characteristic leakage current versus time for a DEA during testing

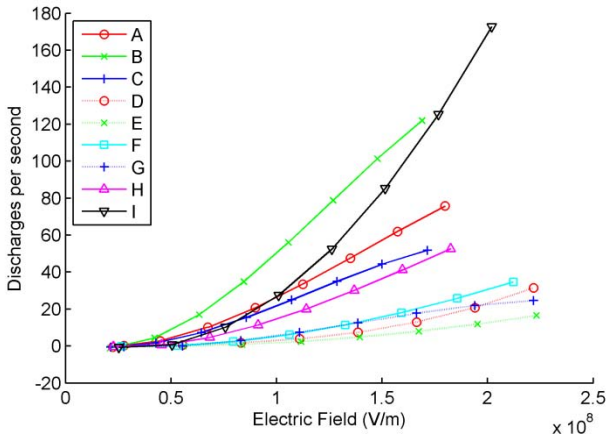

Figure 14: Electric field versus partial discharge event rate for the 9 DEA tested

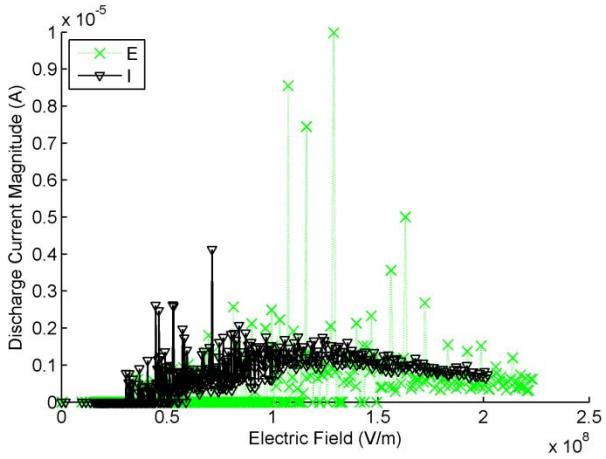

Figure 15: Magnitude of partial discharges versus electric field for a DEA that did not fail during testing (Sample E), and a DEA that did fail (Sample I).

DISCUSSION

Finding an online method for determining when a DEA is near the point of failure has important implications for DEA reliability. At high electric fields device reliability is poor, largely due to the inherent defects in the ultra-thin polymer membranes used in the fabrication of DEA. Spatial variability in the characteristics of the DEA suggests that its breakdown strength is best described by a statistical distribution rather than a specific electric field. Due to this uncertainty DEA are often operated at electric fields far below the maximum levels reported in the literature. This is further complicated by evidence to suggest that the breakdown strength of polymers is a dependent on both the magnitude of the applied electric field and the length of time it is applied (c.f. [7, 8]). Self-clearing electrodes can greatly

improve the operating life of the DEA[6], but with each full breakdown event the active volume of the DEA decreases and a mechanical weak point is created in the DEA membrane.

From Figure 10 it is very clear there is very little spread across all of the DEA tested with regard to the relationship between electric field and area stretch ratio. This highlights the fundamental mechanical repeatability of DEA despite the fact that each of the DEA was fabricated by hand and subject to experimental variability. This consistent behaviour however masks what is happening below the surface. From the other results it can be seen that despite the consistent mechanical behaviour there is significant variability between DEA with regard to leakage current and partial breakdown events.

There is a relatively large variation in the leakage current measured through the dielectric membrane at high electric fields as shown in Figure 11. The most likely explanation for this difference in leakage current is a variable density of inconsistencies such as microscopic voids or foreign particles within the membrane, or localized variations in the thickness of the membrane. Encouragingly, the results indicate a potential relationship may exist between the nominal power dissipated by the DEA at a specific electric field and the quality of the DEA. For example, based on the results shown in Figure 11 a curve formed by the aggregation of data from Samples D, F, and G could represent a boundary between safe operation and over-stressing the DEA. Five DEA that exhibited leakage current and power dissipation per unit area were well above this curve, and failed before the 3000V test limit was reached. One DEA exhibited leakage current well below this curve and did not fail. Of the three DEA clustered around the boundary, two did not fail, and the one that did fail reached the highest electric field of the six failed DEA.

The most interesting result however is that five of the six DEA that failed early exhibited a much higher frequency of partial breakdown events as the electric field increased than the three DEA that did not fail (Figure 14). The sixth DEA (Sample F) was the best performing of the DEA that did fail, and also exhibited a higher rate of discharge events than the three DEA that did not fail, albeit by a smaller margin than the other five. Indeed the only characteristic separating the Sample F from two DEA that did not fail (Samples D and G) was a higher rate of partial discharges at high electric fields. It can also be seen by comparing the data in Figure 14 and Figure 15 that there is a significant difference in characteristics of the partial discharge events between the DEA that failed and those that did not. The DEA that did not fail exhibited much larger, but much less frequent partial discharges. Conversely, the DEA that did fail exhibited much smaller but much more frequent partial discharge events. This is to some degree counter-intuitive; should larger partial discharges not have a higher probability of causing more damage and leading to full dielectric breakdown?

Rapid low amplitude discharges imply some region of the DEA membrane, most likely about a defect, is at its dielectric strength limit, with each discharge relieving the electrical stress sufficiently to prevent full breakdown, but only a very small increase in voltage is required to initiate another partial discharge event. It is not clear whether this causes an accumulation of damage to the dielectric that ultimately results in failure, or whether this behaviour is simply an indicator that the limit is approaching. The DEA that did fail typically had relatively high power dissipation for a given field, thereby potentially requiring a smaller disturbance to push them beyond the thermal runaway threshold. The high frequency of partial discharges could have served to produce this disturbance and push the equilibrium temperature of the membrane beyond what is stable. The DEA that did not fail exhibited a much lower mean leakage current for a given electric field combined with a lower frequency of discharge events, suggesting that despite more energy being involved in each event, the equilibrium temperature remained below the point at which runaway would occur.

Clearly further work is required to develop a better understanding of the effects observed in this experiment. The results suggest some relationship does exist between the leakage current, the number of partial discharge events, and the quality of the DEA. The DEA are clearly differentiable, even at electric fields well below that at which the worst performing DEA failed, and therefore a simple, non-destructive quality control test for newly fabricated DEA could be developed based on these observations.

However, can leakage current be used to detect when a DEA is about to undergo breakdown? More information is required. Based on the data from these experiments no single metric presented in this paper is sufficient in itself to serve as a general purpose indicator of impending dielectric breakdown. Of the DEA that failed, the measured leakage current exhibited a sharp increase at the point of dielectric breakdown that typically occurred over a time scale of 100-200μs. However, there was little to distinguish the initial stages of a partial breakdown event and full dielectric breakdown. In a real system this severely constricts the time available to take corrective action upon its detection. Prior to this breakdown point there was no characteristic behaviour observed in any of the other measured parameters that was common to all of the DEA that failed (i.e. changes in power dissipated per unit area, or discharge events per second). The DEA that failed did exhibit higher nominal leakage current and discharge events per second for a given electric field, but there was no single limit that would ensure all these DEA were being driven to their respective maximum potentials.

Future work will give insight into determining the combinations of measurable parameters that will indicate imminent dielectric breakdown. For example it is unclear what the long term effects of multiple partial discharge events are; do they result in cumulative damage to the DEA that ultimately leads to failure, or can they be sustained indefinitely? Similarly how does the magnitude of the nominal leakage current affect the performance of the DEA over time? It is also important to examine the influence of electrode area on the characteristics of the leakage current. The size of the breakdown zone required to disable the DEA does not change as the area of the electrodes increases, which may mean

any localized tell-tale warning signs of dielectric breakdown are drowned out by the increased conductivity of the DEA as a whole. Mechanical properties must also be taken into account and different initial stretch ratios for the DEA membrane must be tested. In these experiments for example the DEA underwent active area stretches in excess of 2, taking the overall area stretch ratio (pre-stretch plus active stretch) of the membrane to more than 32, which is nearing the upper limit of 36 for VHB4905/4910 tape proposed by Plante[9].

CONCLUSIONS AND FUTURE WORK

In this paper we investigated the behaviour of leakage current through the VHB4905 dielectric membrane of circular DEA as the applied electric field was increased. For the nine DEA tested, five of the six DEA that underwent full dielectric breakdown exhibited significantly higher nominal leakage current for a given electric field compared to the three that did not break down, and all six of the DEA that failed exhibited considerably more frequent partial discharge events that those that didn't. The results indicate monitoring the leakage current of a DEA when subjected to a moderate electric field allow the quality of the DEA to be determined.

The results of this paper however reveal that when viewed individually, nominal leakage current, nominal power dissipated per unit area, or partial discharge events do not exhibit any characteristic behaviour at the point of dielectric breakdown that would provide a reliable indication of impending breakdown for different VHB4905 DEA. It is unclear whether the full dielectric breakdowns observed were primarily the result of thermal instability, the gradual accumulation of damage due to the partial discharge events, mechanical overstressing, or some combination of two or more of these mechanisms. Further characterization of VHB4905 DEA for a wider range of configurations will improve this situation, in particular examining the long term effects of leakage current and partial discharge events on DEA performance. Furthermore the impact of the scale of the DEA and the pre-stretch ratio on these parameters needs to be investigated to gain insight into what combination, if any, of these parameters or others can be used to give sufficient warning of dielectric breakdown that it can be avoided.

ACKNOWLEDGMENTS

The authors would like to thank the Auckland Bioengineering Institute of the University of Auckland, NZ, and the USAF Asian Office of Aerospace Research and Development for financial support.

REFERENCES

1. Madden, J.D.W., Vandesteeg, N.A., Anquetil, P.A., Madden, P.G.A., Takshi, A., Pytel, R.Z., Lafontaine, S.R., Wieringa, P.A., and Hunter, I.W., "Artificial muscle technology: Physical principles and naval prospects," IEEE Journal of Oceanic Engineering 29(3), 706-728 (2004).
2. Kofod, G., "Dielectric Elastomer Actuators," PhD thesis, Risø Technical University of Denmark, (2001).
3. Dissado, L.A., Fothergill, J.C., [Overview of electrical degradation and breakdown], in Electrical Degradation and Breakdown in Polymers, G.C. Stevens, Editor. Lightning Source UK, Milton Keynes. 49-68 (2008).
4. Bauer, S. and Paajanen, M., "Electromechanical characterization and measurement protocol for dielectric elastomer actuators," in Smart Structures and Materials 2006: Electroactive Polymers and Devices 6168 (2006).
5. Gisby, T.A., Xie, S., Calius, E.P., and Anderson, I.A., "Integrated sensing and actuation of muscle-like actuators," in Smart Structures and Materials 2009: Electroactive Polymer Actuators and Devices 7287, 728707 (2009).
6. Yuan, W., Brochu, P., Zhang, H., Jan, A., and Pei, Q., "Long lifetime dielectric elastomer actuators under continuous high strain actuation," in Smart Structures and Materials 2009: Electroactive Polymers and Devices 7287, 72870O (2009).
7. Dissado, L.A., Fothergill, J.C., [Statistical features of breakdown], in Electrical Degradation and Breakdown in Polymers, G.C. Stevens, Editor. Lightning Source UK, Milton Keynes. 319-355 (2008).
8. Keplinger, C., Kaltenbrunner, M., Arnold, N., and Bauer, S., "Capacitive extensometry for transient strain analysis of dielectric elastomer actuators," Applied Physics Letters 92(19) (2008).
9. Plante, J.S., "Dielectric Elastomers for Binary Robotics and Mechatronics," PhD, Massachusetts Institute of Technology, (2006).

Appendix 3:

Here we have appended a draft paper to be presented at SPIE Smart Structures/NDE Electroactive Polymers and Devices Conference, San Diego March 6-10 2011:

Development of pain detection circuit and real time demonstration

Introduction

In our previous study, experimental data pertaining to leakage current through the dielectric membrane of Dielectric Elastomer Actuator(s) (DEA) [1] was collected under controlled laboratory conditions. There were elements of post-processing that precluded implementation of a real-time pain parameter. The results clearly indicated merit in developing a better understanding of the behaviour of leakage current so as to prevent failure in DEAs. However, to be meaningful it is necessary to measure leakage current in real-time, for there is a significant difference between sensing leakage current under controlled conditions and sensing leakage current in real-time and 'in the field'.

We have a proprietary algorithm for measuring the capacitance of a DEA and the nominal leakage current through the dielectric membrane whilst it is being actuated. With the support of the USAF AOARD we have developed a prototype circuit for its implementation. Using this circuit we conducted experiments to evaluate its performance as a predictor of dielectric breakdown in DEA. In particular we have characterised the behaviour of the leakage current as measured in real-time for the period leading up to dielectric breakdown. In this report we present a method for real time 'pain' detection based on leakage current monitoring. We intend to present the information contained in this report at the annual SPIE Electroactive Polymers and Devices (EAPAD) Conference in San Diego, CA, USA.

Materials and Methods

The experimental system consisted of expanding dot DEA with supporting electronics. We describe below:

- The DEA used for testing
- Circuit design criteria
- Self-sensing circuit design
- The experimental configuration

Actuator system with model

Five DEA (Samples A-E) were fabricated from sheets of 3M VHB4905 tape stretched equibiaxially to 16 times their original area and bonded to a rigid circular support frame (Figure 1). Each support frame had an internal aperture with a diameter of 100mm. Circular electrodes with an approximate diameter of 25mm were applied to opposing sides of the stretched membrane. Nyogel 756 electrically conductive carbon loaded grease was used as the electrode material. Flexible copper traces were used to connect the electrode area to the points on the edge of the support frame that could be connected to external circuitry. The viscosity of the carbon grease was sufficient to hold the copper trace in place without the copper coming into direct contact with the membrane. A schematic representation of the DEA is shown in Figure 2.

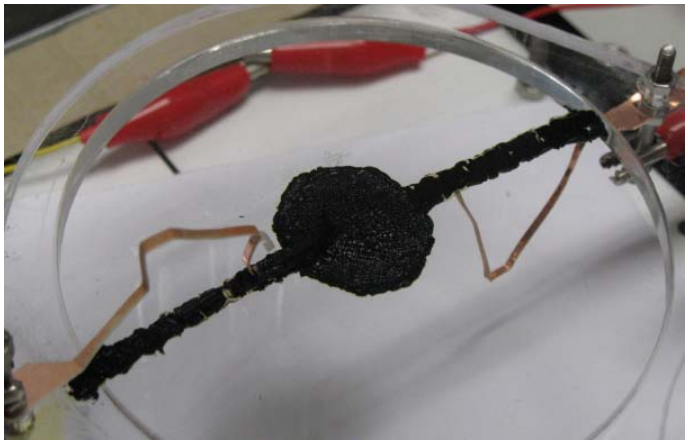

Figure 1: Photo of a DEA used in testing

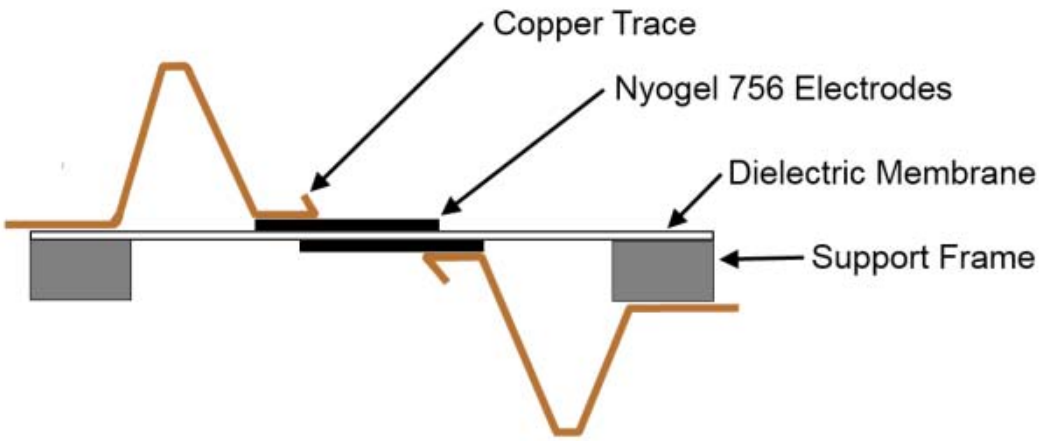

Figure 2: Schematic cross-section drawing of the DEA used for testing

A simple model of the DEA consists of a variable capacitor (*C*) in parallel with a an variable Equivalent Parallel Resistance (EPR) representing the dielectric membrane (R_{EPR}), both of which are in series with a variable Equivalent Series Resistance (ESR) representing the electrodes (R_{ESR}) (Figure 3).

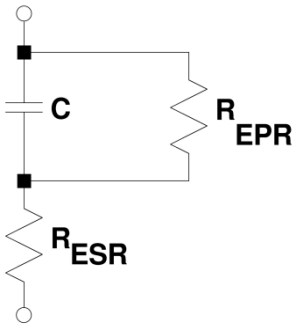

Figure 3: Lumped circuit model of a DEA

For small DEA it is possible to fabricate the electrodes such that R_{ESR} is negligible and can be assumed to be zero. Given that we are investigating leakage current**,** R_{EPR} is our main parameter of interest.

The total current through a DEA is the sum of the current due to the capacitance charging/discharging, the current induced due to the capacitance changing, and leakage current through R_{EPR} (Equation 1) [2].

$$i_{total} = C\frac{dV}{dt} + \frac{dC}{dt}V + i_{EPR} \tag{1}$$

We have an algorithm for decomposing the total current through a DEA into these three components that uses Pulse Width Modulation (PWM) to simultaneously actuate and provide the correct stimulus for sensing the electrical characteristics of a DEA.

The DEA acts as a low pass filter to the PWM signal due to its predominantly capacitive nature. When the period of the PWM signal is small relative to the electrical and mechanical time constants of the DEA, the PWM signal is transformed into an average voltage proportional to the duty cycle of the PWM. The rapid switching of the signal also generates small scale oscillations in the voltage across the DEA. The actuation of the DEA is proportional to the average voltage, whilst the small scale oscillations enable the electrical parameters of the DEA to be determined.

The voltage difference between the positive and negative terminals of a DEA is the sum of the voltage cross the capacitive component and the product of the series current and R_{ESR}. The small DEA with their thick carbon grease electrodes and highly conductive wire traces for the external electrical connections rendered R_{ESR} sufficiently small that the voltage drop across the electrodes can be ignored.

Circuit design criteria

At the heart of any DEA driver circuit is a high voltage power supply. Low power DC-DC converters typically consist of a voltage controlled oscillator supplying an AC signal into a small transformer, the output of which is further amplified and rectified by a Villard Cascade (Figure 4). These devices are capable of generating a wide range of voltages, however they are typically capable of very low output currents (<1mA). This is perfectly adequate for small DEA, however care must be taken not to exceed the rated current of such devices or risk the output voltage sagging significantly. Furthermore, the rectification of the output stage limits the ability for the DC-DC converter to sink current.

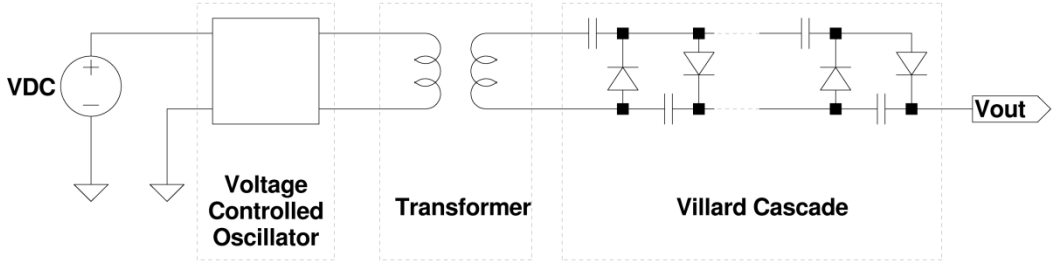

Figure 4: Schematic drawing of a typical low power DC-DC Converter

We paired a DC-DC converter with a high speed, high voltage opto-coupler (OC100HG, Voltage Multipliers Inc). The high speed at which the opto-coupler can switch makes PWM of the high voltage signal feasible. Furthermore, the current flowing from the DC-DC converter to the load is proportional to the input current supplied to the opto-coupler, thus the opto-coupler acts as a variable current throttle that ensures the rated current output of the DC-DC converter is not exceeded. This also provides an additional benefit for the future: in devices that have multiple degrees of freedom, appropriate tuning of the amplitude and the phase of the PWM signals mean a single DC-DC converter can be connected to multiple DEA via multiple opto-couplers, yet a different voltage can be applied to each DEA. A single power supply can therefore be used to control multiple DEA independently. This effectively decouples the DEA from the dynamics of the DC-DC converter. Such a configuration necessarily requires a separate discharge path for the DEA being controlled, however this can easily be achieved by passive or active means (e.g. a resistor connected in parallel with the DEA or a second switch dedicated to discharging the DEA).

The rapid switching of the PWM signal induces oscillations to the voltage across the DEA that make sensing the electrical characteristics of the DEA possible. For this approach to be effective however it is necessary to make the period of the PWM signal small relative to the electrical and mechanical time constant of the DEA. By doing so the degree of actuation is solely related to the average voltage, and the small scale oscillations of the DEA are not reproduced mechanically. This is heavily dependent on the material from which the DEA is fabricated. However keeping the period of the PWM signal short limits the peak-to-peak swing of the instantaneous voltage across the DEA (see Figure 5). This reduces the variation in the electrostatic pressure applied to the DEA over the course of a single cycle of the PWM signal.

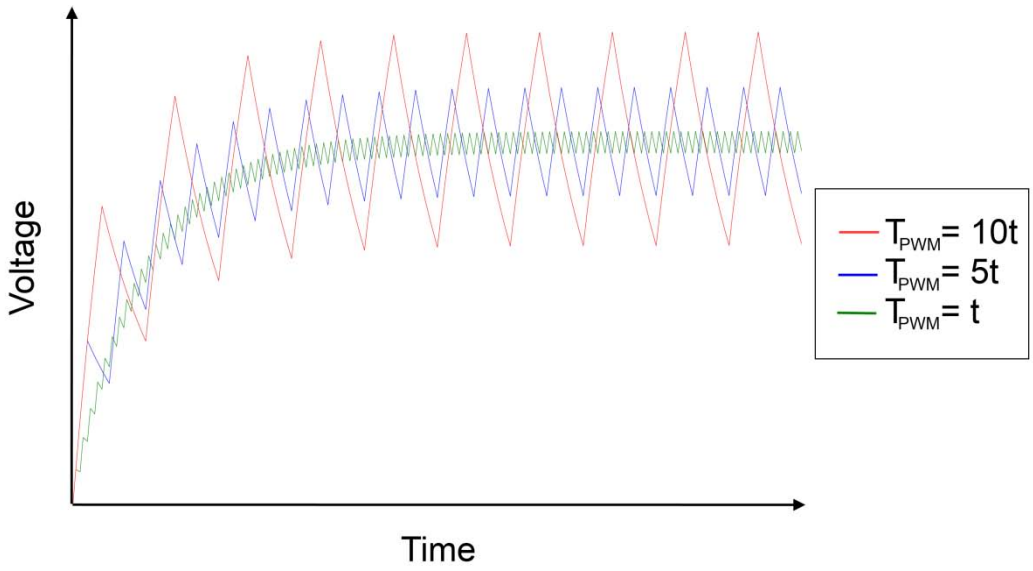

Figure 5: Effect of PWM period on the peak-to-peak voltage swing across a DEA

From a mechanical standpoint it is desirable to reduce the oscillations in the voltage across the DEA as much as possible, but there is a trade-off with regard to the other functions the PWM signal performs. Some degree of oscillation is required in order to sense the electrical characteristics of the DEA. Furthermore, in order to sense these characteristics data in the form of sampled voltage levels must be acquired e.g. using an Analog-to-Digital Converter (ADC). There is a limit to the maximum rate at which an ADC can accurately sample voltage data. Thus there exists a design trade-off with regard to setting the frequency of the PWM signal: it must be fast enough to exceed the mechanical response of the DEA, but not so fast that it becomes impractical to acquire and process the feedback data necessary to estimate its electrical characteristics.

Self-sensing circuit design

In order to estimate DEA capacitance and leakage current through the dielectric membrane, it is necessary to know the series current (i.e. i_{total} from Equation 1) through the DEA and the voltage (V) between its positive and negative terminals. Good quality feedback signals are required; the sensing circuit must operate in a high voltage, low current regime, and as such is particularly susceptible to noise generated by sources both internal and external to the sensing circuit. Good circuit design therefore is essential. Minimising the length of circuit tracks and buffering signals where possible greatly improves noise rejection. Hardware and software filtering are also useful, but great care must be taken to ensure that the filters do not interfere with the circuit's ability to capture the characteristic features of the signals of interest.

Several iterations of a prototype circuit were designed to implement the self-sensing method. The final design is presented in Figure 6. An OC100HG opto-coupler driven by a PWM signal regulated the current flow from the high voltage supply to the load. A 100MOhm:120kOhm resistor ladder between the positive terminal of the DEA (Node1) and ground was used to step down the voltage at the positive terminal for measurement. This resistor ladder also provides a passive discharge path for the DEA. The negative terminal of the DEA (Node2) was connected to a 1.2V reference voltage rail via a 30kOhm resistor. Having a positive reference rail enabled the circuit to be designed such that V_2 remained positive relative to the ground potential for the entire range of expected series currents. This eliminated the need to create a power rail with a negative potential, and shifts the voltage of the signal to a range that is suited to the Analogue-to-Digital Converter (ADC) inputs of a microcontroller.

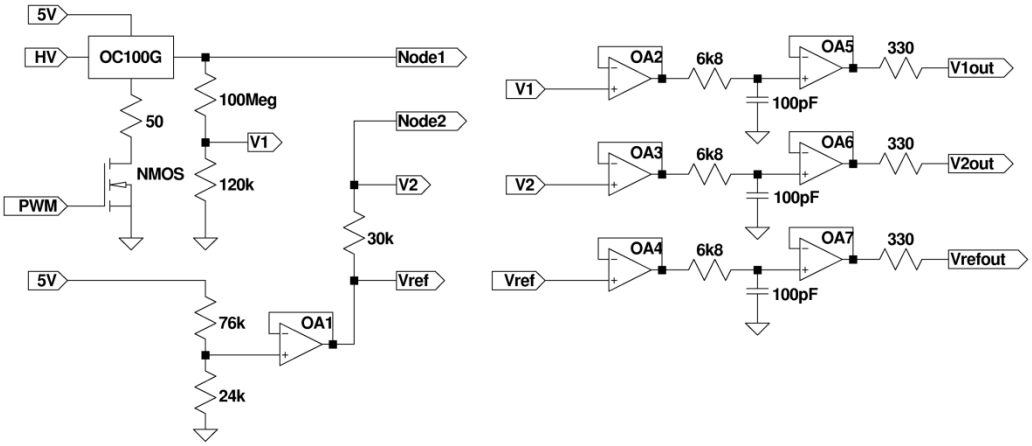

Figure 6: Schematic representation of a simple driver and sensor circuit for a DEA

The signals of interest were the voltage across the 30kOhm resistor (V_2–V_{ref}) and the voltage across the 120kOhm resistor (V_1). A quad package rail-to-rail operational amplifier (OPA-4344, Burr-Brown) placed as close as possible to the sense resistors was used to buffer each of the signals. The very small bias current at the input terminals of the OPA-4344 (max. ±10pA) ensures the act of measuring the signals has a negligible impact on the behaviour of the system. Each signal was filtered using a simple single pole RC filter before being buffered by a second OPA-4344 prior to being transmitted to an ADC. The active nature of the outputs of the amplifiers act to reject noise picked up by the transmission path between the amplifier and the ADC.

Experimental Setup

To evaluate the performance of our real-time leakage current sensing we must be able to independently verify the leakage current for a given state of operation. In [2] however we showed that despite several different DEA exhibiting nearly identical relationships between area stretch and applied electric field, there was a large variation in the relationship between leakage current and applied electric field. Experimentation was therefore split into two stages: “mock” DEA circuits were constructed from fixed value components to verify the leakage current measurements made using our prototype circuit; and expanding dot DEA were used to characterize the DEA Capacitance and sensing of leakage current through the membrane in real-time.

Several mock DEA circuits were constructed using nominally fixed value components to validate the real-time sensing of leakage current. The circuits consisted of a high voltage capacitor and a range of resistors representing the EPR of the DEA. This enabled the circuit to be broken down into its constituent parts so that they could easily be tested independently.

Three values of R_{EPR} were tested: infinity (i.e. no resistance in parallel with the capacitor), 300MΩ, and 150MΩ. A 4kV DC signal was applied to the HV terminal of the prototype circuit using a Generation 2 Biomimetics Laboratory EAP Controller. A PWM signal with an initial duty cycle of 10% was then applied to the DEA. The amplitude of the PWM signal was tuned such that the current through the opto-coupler was approximately 120μA when the PWM signal was on, and <1μA when the PWM signal was off. The duty cycle was then increased in 5% increments every 10 seconds until the mean voltage across the DEA reached 3kV. The circuit was calibrated by assuming the estimated leakage current for the $R_{EPR}=\infty$ case represented the “zero current” curve.

Once validated, the circuit was used to characterize the behaviour of the leakage current through the membranes of several expanding dot DEA as measured in real-time. A 4kV DC signal was applied to the HV terminal of the prototype circuit. A PWM signal with an initial duty cycle of 10% was applied to the DEA. The duty cycle was then increased in 1% increments every 10 seconds until the DEA failed. During this period, the mean voltage across the DEA, the capacitance of the DEA, the nominal leakage current through the DEA, and the amplitude of the noise in the nominal leakage current were estimated using our self-sensing algorithm. Note the current due to the rate of change of the capacitance is sufficiently small for the test conditions that

it can be ignored; however in future tests the rate of change of capacitance can be estimated using the time history of the capacitance.

Results

The results of the estimation of the leakage current for the mock DEA circuits after the self-sensing circuit has been calibrated are presented in Figure 7. Note the blue lines indicate the expected values for the leakage current based on the applied voltage and the size of the resistor used for R_{EPR}. The estimated leakage current data is overlaid as red crosses. This data has been downsampled to improve readability.

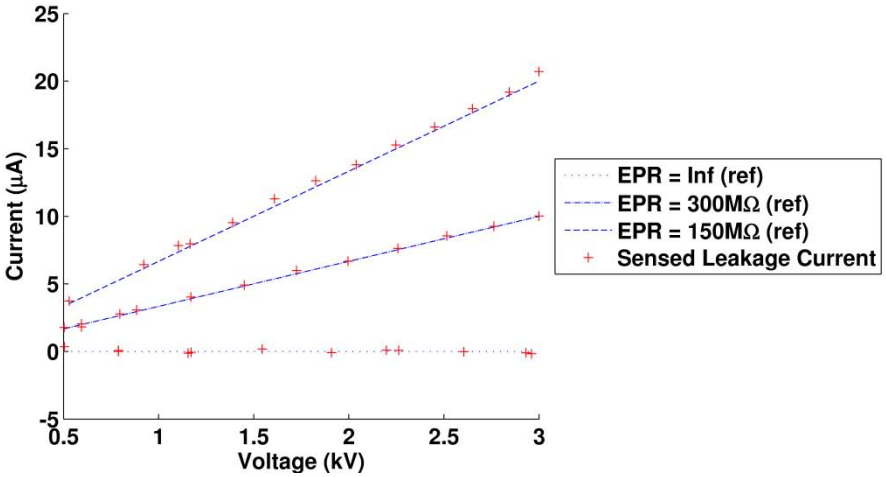

Figure 7: Predicted leakage current (blue lines) and leakage current as estimated using self-sensing (red crosses)

The test DEA showed exceptional resilience when subjected to high actuation voltages. At very high strains however cracks appeared in the electrode and it ceased to be a continuous layer (see Figure 8).

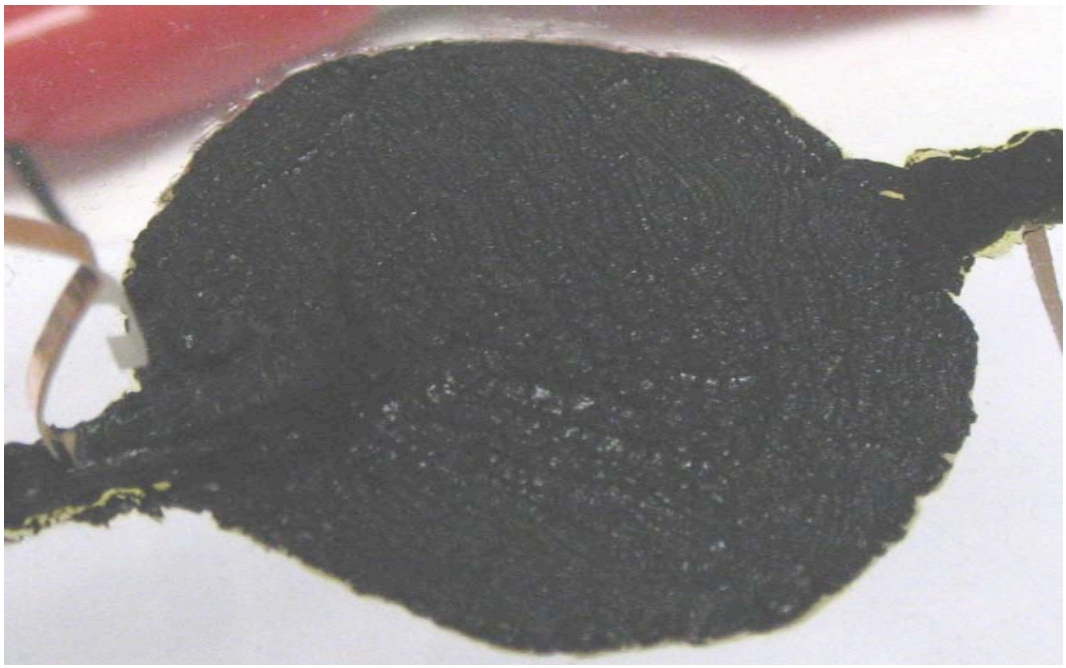

Figure 8: Close up of the cracks beginning to appear in the DEA electrode at high active strains

For each cycle of the PWM signal, the mean voltage across the DEA was measured. The mean voltage for the entire test cycle is shown in Figure 9. In Figure 10 a close-up of the mean voltage with respect to time of the latter portion of the test cycle is shown. The mean voltage drops away sharply when full dielectric breakdown occurs. Note the mean voltage is asymptotic because the

maximum input current is restricted to ~120μA whilst the discharge current during the off portion of the PWM cycle is proportional to the voltage across the DEA.

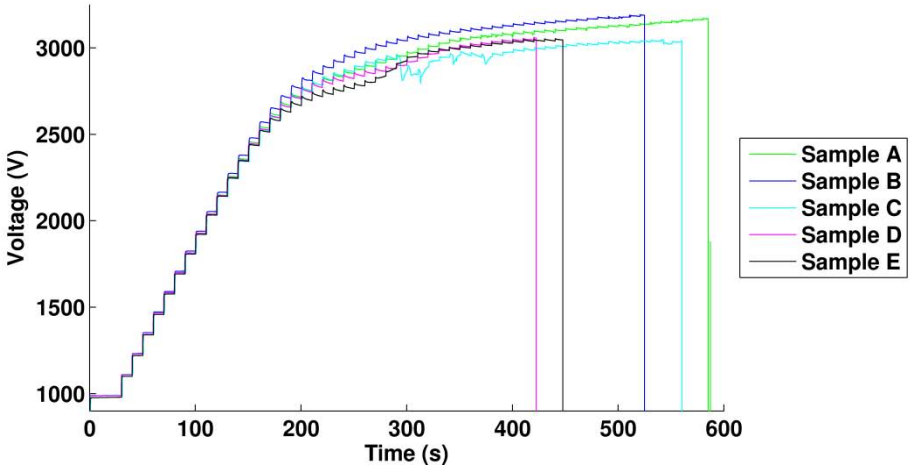

Figure 9: Mean DEA Voltage versus time for each test DEA

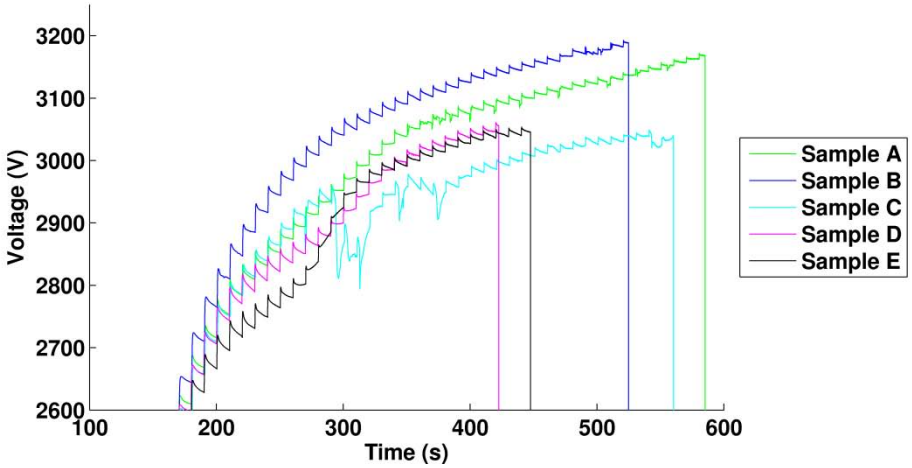

Figure 10: Close up view of the mean DEA voltage for *V>2600*

Figure 11 displays the capacitance as measured by the self-sensing process. In Figure 12 the measured leakage current with respect to time is presented. Note in both Figure 11 and Figure 12 the vertical lines at the end of each curve represent breakdown conditions. The amplitude of the noise in the leakage current measurements is shown in Figure 13 (note: the data in this figure has downsampled for readability).

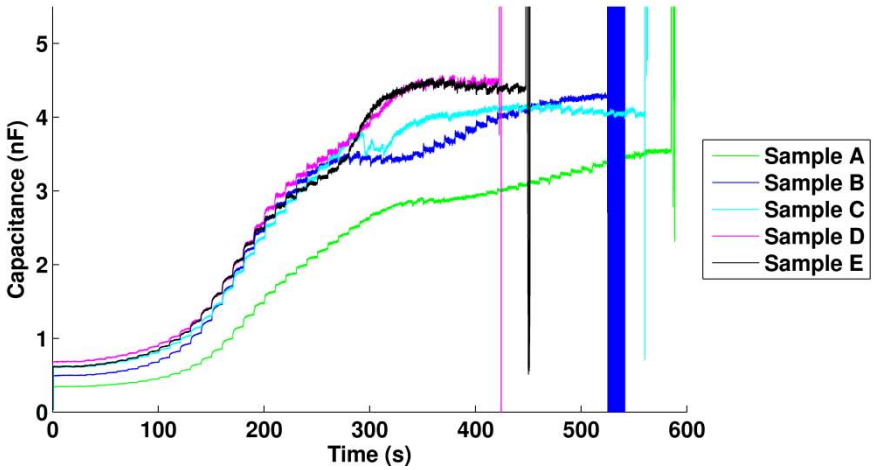

Figure 11: DEA capacitance versus time

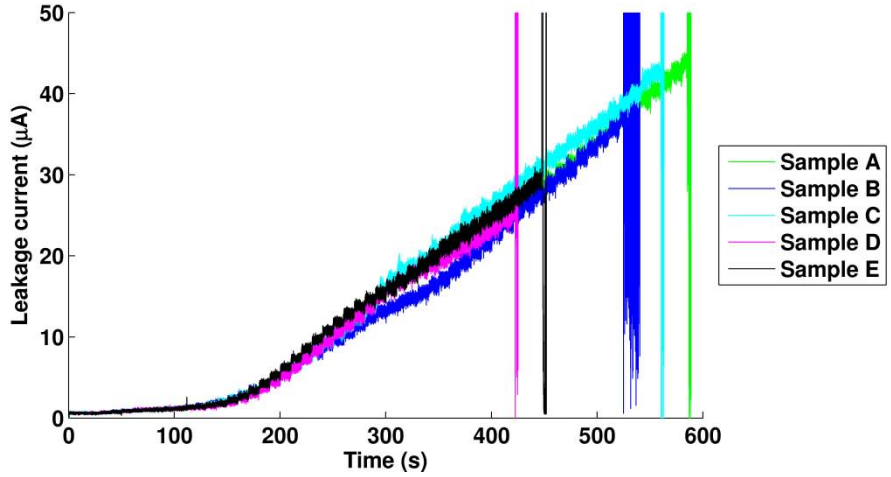

Figure 12: Estimated leakage current versus time for each test DEA

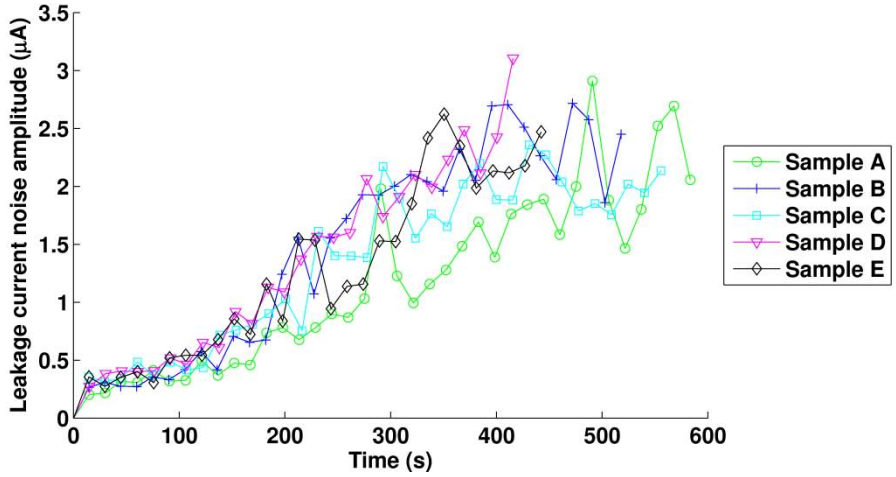

Figure 13: Amplitude of noise in estimated leakage current

Discussion

The results of the experimental validation indicate our self-sensing algorithm provides a good estimation of leakage current in real-time (Figure 7).

We can clearly see from Figure 12 that the estimated leakage current exhibits a much smaller degree of variation when compared with the data presented in our previous study [1]. We attribute this to improvements in the fabrication process. In our earlier experiments a fine hair paint brush was used to apply the carbon grease. Although the hairs are highly flexible, we feel it is possible for tips of the hairs to damage the surface of the membrane, creating a weak point in the dielectric membrane. Alternately, the hairs could break off and be left within the grease. The tips of any fibre-like particles left behind act to concentrate the electric field, creating a local region that is more susceptible to dielectric breakdown. By using the rubber-tipped colour shaper these potential problems have been avoided.

Improvements in reliability resulted in greater active strains for the 5 test DEA when compared with the test DEA fabricated earlier [1]. In the current experiments, the peak area strain ranged from 150-220% for the 5 test DEA, whereas in [1] peak area strains were limited to 100-150% for the 9 DEA tested. This impressive active strain brought to light issues with regard to the electrode material. At very high strains the surface of the electrode began to crack up and form islands of conductive material (see Figure 8). This creates non-uniformity in the resistance of the electrodes. In extreme cases it may result in portions of the electrode becoming electrically isolated. This could explain the variations observed in the measured capacitance of the DEA (Figure 11, 200-350 seconds). As the DEA expands, small local regions that have effectively become isolated no longer contribute to additional expansion or they contribute in a reduced capacity as the mean voltage is

increased. We have assumed the overall equivalent series resistance of the DEA remains small, however this effect does warrant further investigation.

For all five actuators the estimated capacitance reached a plateau, and in two cases (Samples C and E) had begun to decrease in the period leading up to breakdown i.e. each DEA was substantially at its maximum active displacement. The consistency of this effect is promising however this may have been affected by the cracking of the electrodes at very high strains. Furthermore in a practical application this effect could be recreated by a blocking force imposed by an external load, thus further testing is required to explore the significance of this result.

In line with previous experiments, partial discharges appear to be a notable indicator of impending dielectric failure. In our earlier study [1], we showed that DEA typically exhibit frequent small partial discharge events with occasional much larger partial discharges prior to breakdown. Significant partial discharges present as sharp drops in the mean voltage across the DEA. In the current experiments, Samples A, B, and C clearly demonstrated significant partial discharges as the mean applied voltage exceeded 2.6kV (Figure 10). Most importantly, the partial discharges occurred several seconds before dielectric breakdown. Furthermore, when correlated with the measured capacitance, the significant partial discharges corresponded to the measured capacitance effectively reaching a plateau, or in the case of Sample C the measured capacitance was decreasing. Thus these precursors to breakdown occur when the DEA is substantially at its maximum active strain. Samples D and E however do not exhibit the hallmarks of significant partial discharge events in the period leading up to full breakdown. When we look at capacitance (Figure 11) we can see that, like Samples A-C, the measured capacitance plateaued for Sample D and then began decreasing. In the case of Sample E this happened several seconds before full dielectric breakdown.

While significant partial discharge events are clearly evident in the mean voltage across the DEA, the design of the self-sensing circuit prevented the direct measurement of high frequency, low charge discharge events. This is due to at least two reasons. Small partial discharge events do not have a significant impact on the DEA voltage. The signal conditioning filters on the output signals of the self-sensing circuit also attenuate small individual partial discharge events. Numerous partial discharge events however will affect the estimated leakage current. Whilst attenuated, they will appear as noise in the signals used to estimate leakage current. If we assume some deviation occurs in the magnitude and frequency of the small partial discharge events between cycles of the PWM input signal, this will manifest as noise in the estimated leakage current. This is demonstrated in Figure 13. Despite each of the five test DEA failing at different voltages, times, and capacitances, the noise in the estimation of the leakage current at breakdown was similar for all five. Each failed when the amplitude of the noise in the estimated leakage current reached approximately 2-2.5μA.

Conclusions

We have successfully designed, built, and tested a prototype circuit for implementing our self-sensing algorithm. The circuit accurately predicted the leakage current through several mock DEA circuits in real-time without requiring off-line processing of the feedback data.

We observed substantial improvements in the overall performance of DEA, compared with our earlier work. We believe this is associated with use of a rubber tipped colour shaper to apply the electrodes instead of a paint brush. If so, this highlights the important role of the electrode fabrication process for DEA reliability.

Our experiments and analysis indicate that a practical pain parameter should be based on multiple measurable electrical parameters: the mean voltage across the DEA; the capacitance of the DEA; and the amplitude of the noise in the estimated leakage current through the dielectric membrane.

Significant partial discharges have a noticeable effect on the mean voltage, and in three of the five actuators tested they were observed several seconds before full dielectric breakdown occurred,

For DEA subjected to a constant load, the estimated capacitance reached a plateau, and in two cases had begun to decrease, shortly before full breakdown. The estimated capacitance indicates the DEA is near its maximum active strain limit. Further work is required to explore the significance of this result for DEA subjected to variable loads.

All five actuators failed when the mean amplitude in the noise in the estimated leakage current reached a level of approximately 2.25μA. This is in spite of the fact that each of the five test DEA failing at different voltages, times, and capacitances.

Future Work

Several important avenues for future work arise from the results of our current experiments. The behaviour of the electrodes at very high strains suggests a means for measuring the equivalent series resistance of a DEA that will provide valuable feedback information. Resistance sensing will potentially enable the measurement of mechanical strain. It will also enable the voltage drop across the electrodes to be estimated, which we have to this point assumed to be negligible.

It will also be important to test the self-sensing process on DEA that are subjected to external disturbances. In practice "pain" is not necessarily limited to cases where the DEA is at its maximum extension. External loads affect the equilibrium position of the DEA, thus it is necessary to examine their influence on the parameters of interest we have identified.

Pain sensing will substantially improve reliability and range of artificial muscle devices. In many applications a significant safety factor is used to determine the maximum electric field applied to a DEA. For DEA fabricated from VHB4905 a typical limiting value is 80MV/m. Based on our experiments, the worst performing DEA (Sample D) sustained an electric field in excess of 240MV/m before failing. This represents an active pressure 9 times greater than if a typical safety factor is imposed on the maximum electric field applied to the DEA. Clearly there is significant benefit to sensing pain in DEA.

Acknowledgements

The authors would like to thank the USAF Asian Office of Aerospace Research and Development for financial support.

References

1. T. A. Gisby, S. Q. Xie, E. P. Calius, and I. A. Anderson (2010), *Leakage current as a predictor of failure in dielectric elastomer actuators*, Proc. SPIE 7642, Article No. 764213, DOI:10.1117/12.847835
2. T. A. Gisby, S. Q. Xie, E. P. Calius, and I. A. Anderson (2009), *Integrated sensing and actuation of muscle-like actuators*, Proc. SPIE 7287, Article No. 728707, DOI:10.1117/12.815645